

# FAULT TOLERANT CONTROL FOR SERIES COMPENSATORS FOR POWER SYSTEM STABILITY IMPROVEMENT

**Mrs. R.Naveena Bhargavi<sup>1</sup>, Dr. S.Venkateshwarlu<sup>2</sup>, Mrs. M.Rajasree<sup>3</sup>**

*<sup>1</sup>Associate Professor, <sup>2</sup> Professor & HOD, <sup>3</sup> Assistant Professor,  
EEE Department, CVR College of Engineering , Hyderabad, (India)*

## ABSTRACT

*This paper presents a fault –tolerant indirect adaptive neuro-controller (FTNC) for controlling a Series Compensator, which is connected to a power network. The FTNC consists of a sensor evaluation and restoration scheme (SERS), a radial basis function neuro-identifier (RBFNI) and a radial basis function neuro-controller (RBFNC). The SERS is designed using the auto-associative neural networks(auto-encoder). This FTNC is able to provide efficient control to the Series Compensator when single or multiple crucial sensor measurements are unavailable. The validity of the proposed model is examined by simulations inMATLAB/SIMULINK environment.*

**Keywords:** *CSC, TCSC, Fault –Tolerant Control, Neural Networks, Series Compensator.*

## 1.INTRODUCTION

Power utilities of today use a variety of technologies to reduce the impact of disturbances in the power grid, lowering the risk of blackouts. Many of these are commonly referred to as Flexible AC Transmission Systems(FACTS) devices. Two well known FACTS devices are the Thyristor Controlled Series Compensator(TCSC) and the Thyristor Switched Series Compensator( TSSC) belonging to the group of Controlled Series Compensators(CSC). CSC are based on the principle of varying of the power line series reactance in order to control power flows and enhance system stability. The most important phenomena which threaten the stability of power systems are poorly damped low frequency electromechanical oscillations, first-swing instabilities and voltage instabilities.

In terms of the control objectives, various control schemes, based on the conventional linear PI controllers, have been designed for the internal control of the Series Compensator [3]-[6]. From proposed references , the neuro-controller was shown improved transient performance over the conventional linear PI controllers(CONVC).

However, control of nonlinear plants in power systems relies on the availability and the quality of sensor measurements. Measurements can be corrupted or interrupted due to sensor failure, broken or bad connections, bad communication, or malfunction of some hardware or software (these are referred as missing sensor measurements in this paper). If some sensors fail to provide the correct information, the controllers cannot guarantee the correct control behavior, for the plant based on the faulty input data. Therefore, fault-tolerant measurements are an essential requirement for system control. For many systems, certain degrees of redundancy are present among the data collected from various sensors. If the degree of redundancy is sufficiently high, the readings from one or more missing sensors may be able to be accurately restored from those remaining healthy sensor readings. Conventional methods in recovering missing sensor data are based on the analysis of the system model, e.g., the state estimation methods. The drawbacks of these methods have been discussed in [7],[8].

This paper proposes a fault-tolerant indirect adaptive neuro-controller (FTNC) for the internal control of a Series compensator connected to a power network. This FTNC contains a SERS cascaded with a radial basis function neuro-identifier (RBFNI) and a radial basis function neuro-controller (RBFNC), as shown in Fig.1. The RBFNI is trained to provide a dynamic predictive plant model at all times; this plant model is then used for training the RBFNC; the RBFNC in turn generates the control signals to drive the outputs of the actual plant to the desired values [6]. The SERS is used to evaluate the integrity of the crucial sensor measurements that determine the behaviors of the RBFNI and the RBFNC. If one or more sensors are missing, the SERS searches in its input space for the optimal estimates of the missing data. The restored values of the missing data from the SERS, together with the remaining data read directly from the healthy sensors, provide a set of complete inputs to the RBFNI and the RBFNC. This guarantees a fault-tolerant control for the Series compensator. Simulation studies are carried out with single and multiple time varying current sensors missing in order to evaluate the performance of the proposed FTNC scheme.

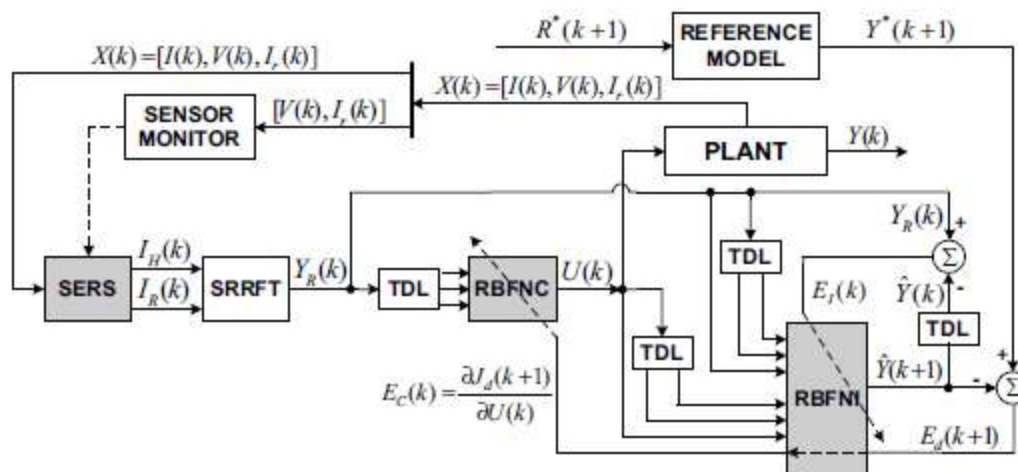


Fig.1.Schematic diagram of the fault-tolerant indirect adaptive neuro-controller(FTNC) connected to the plant: $R^*=[Q^*,P^*]$ ,  $Y^*=[i_q^*,i_d^*]$ ,  $U=[v_{eq}, v_{cd}]$ ,  $Y=[i_q,i_d]$ ,  $Y_R=[i_{qR}, i_{dR}]$ ,  $Y=[i_q^*,i_d^*]$ ,  $I=[i_a, i_b, i_c]$   $V=[v_{ca},v_{cb},v_{cc}]$ , and  $I_r=[i_{ra},i_{rb},i_{rc}]$ . SRRFT means synchronously rotating reference frame transformation.

## II REDUCED GRID MODEL

In order to design a damping controller for inter-area power oscillations, a system model is required. The nature of inter-area oscillations is often such that there is a dominant mode of oscillation which may be poorly damped. With this in mind, a simple way to reduce the total power grid is to approximate the grid as a system of the form seen in Fig.2. The reduced model of the power system using a Center Of Inertia (COI) reference frame consists of two synchronous machines with interconnecting transmission lines. In this work, the model parameters are updated continuously by the controller using the locally measured responses in the CSC line active power( $P_{line}$ ) to changes in the variable series reactance.

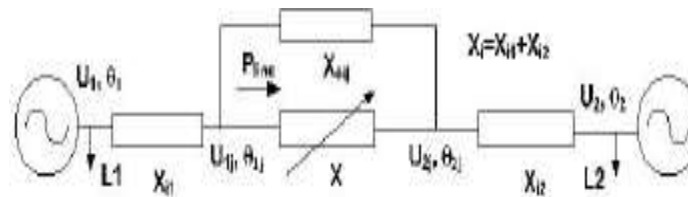


Fig.2 The reduced grid model used by the controller

The line where the CSC is installed is represented by a variable, known reactance  $X$ . The model is characterized by four additional parameters: one series reactance  $X_{1l}$ , one parallel reactance  $X_{eq}$ , the dominant angular frequency of the power oscillation  $\omega$  and the damping exponent of this oscillation mode  $-\sigma$ . The machine terminal voltage phasors characterized by the magnitudes  $U_{1,2}$  and the phase angles  $\Theta_{1,2}$  are assumed to be well controlled and thus constant in magnitude. When applied to real power systems, the model [1] may represent two different grid areas with lumped moments of inertia and their interconnecting power lines. The load in each of these areas is modeled as constant voltage-independent loads.

## III THEORY

### 3.1. Estimation of the reduced model parameters

Since an adaptive control approach is used, the parameters of the grid where the FACTS device is placed are estimated continuously by the controller according to the model of Fig.2. The controller is time-discrete in nature making it possible for the estimation routines to be developed based on the step response of the reduced system in Fig.2 to changes in the CSC reactance. In [1], equations governing the step response in active power on the reactance controlled line when a step in the line reactance is applied to a system at rest were derived. It is also

possible to derive relations for the step response of the system when it is initially subject to an electro-mechanical oscillation. Such relations are used by the controller proposed here to estimate the grid parameters in real-time.

### 3.2 Estimation of the CSC line power frequency content

In order to use the estimation techniques outlined above and to determine the input and timing for the damping controller it is necessary to separate the average and oscillative components of the line active power in real-time. This is done using a Recursive Least Squares (RLS) algorithm [9]. In this paper, the algorithm is used based on the assumption that the line power is composed of a zero frequency component (the average value) and a component which has a known frequency range (the power oscillation frequency). The algorithm utilizes an expected oscillation frequency when no oscillations are at hand. At any event that causes power oscillations, the frequency parameter is adapted to the actual oscillation frequency by a PI-controller. The algorithm gives a real-time estimation of the line average power ( $P_{av}$ ), oscillation amplitude ( $P_{osc}$ ), frequency ( $\omega$ ) and phase ( $\phi_{osc}$ ).

### 3.3. Power oscillation damping

The controller developed here is based on a time-discrete approach to power oscillation damping. The approach is somewhat similar to that of [6]. In [2] it was shown that a power oscillation in a power system characterized by one dominant mode of oscillation can be damped by changing a selected line series reactance in one step of a certain magnitude at a carefully selected time instant. The necessary reactance magnitude can be determined knowing the system parameters according to the model of Fig. 2. It was also shown that a more realistic controller can be built on the principle of (ideally) eliminating the power oscillation in two discrete reactance steps separated in time. This objective can also be met simultaneously as the active power flow on the reactance controlled line is changed to a pre-defined new set-point as shown in [3]. The time instants of the steps must be chosen such that they coincide with peaks (positive and negative) in the power oscillation. This gives a controller with a time-discretization determined by the oscillation frequency.

## IV MULTI-OBJECTIVE CONTROLLER

Now, a controller for power oscillation damping (POD), first-swing stability improvement (FSW) and active power flow control can be designed. The first-swing controller has the highest priority and inhibits the other controller parts if initiated. Generally, a fault in the system first leads to a risk of transient instability which initiates the first-swing controller. When the first-swing controller has performed its sequence there is commonly a power oscillation in the system which is detected by the RLS algorithm. This oscillation triggers the damping controller which has a built-in power flow control feature for fast control of the power on the line after a fault. Since the damping controller/fast power flow controller is only active when power oscillations are present, a separate slow PI-controller is necessary for long-term power flow control. These controllers contribute the terms  $X_{POD}$ ,  $X_{PSW}$  and  $X_{PI}$  to the

reactance of the CSC- $X_{TCSC}$  (Fig.3). All controllers use the CSC line active power ( $P_{line}$ ) or estimations of it as input signals. The first swing controller also uses the CSC line current ( $I_{line}$ ) as an input signal.

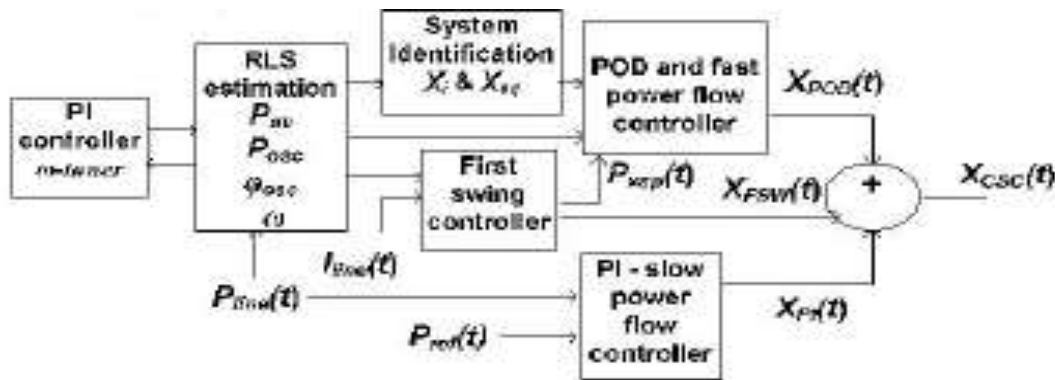


Fig.3: Principal schematic of the CSC controller

## V FAULT-TOLERANT INDIRECT ADAPTIVE NEURO-CONTROLLER

### 5.1. Design of RBFNI and RBFNC

The RBFNI and RBFNC are each a three-layer RBF network with the Gaussian density function as the activation functions in the hidden layer. The overall input-output mapping for the RBF network,  $f: X \in R^n \rightarrow Y \in R^m$  is

$$\hat{y}_i = b_i + \sum_{j=1}^h v_{ji} \exp\left(-\frac{\|x - C_j\|^2}{\beta_j^2}\right) \quad (1)$$

where  $x$  is the input vector,  $C_j \in R^n$  is the center of the  $j^{\text{th}}$  RBF units in the hidden layer,  $h$  is the number of RBF units,  $b_i$  and  $v_{ji}$  are the bias term and the weight between hidden and output layers respectively, and  $y_i$  is the  $i^{\text{th}}$  output. The RBFNI is used to provide a dynamic predictive plant model at all times. This model is then used for training the RBFNC. The RBFNC is used to replace two conventional PI controllers (PI<sub>d</sub> and PI<sub>q</sub>) in Fig. 3. The inputs of the RBFNC are the plant outputs at time  $k-1$ ,  $k-2$  and  $k-3$ . It in turn generates the control signals as the plant inputs in order to drive the plant outputs to the desired values. The detailed design and training process for the RBFNI and RBFNC has been discussed in [6].

### 5.2. Missing Sensor Restoration Algorithm (MSR)

Figure 4 shows the structure of a MSR block [7], [8]. It consists of a dynamic auto-associative neural network (autoencoder).

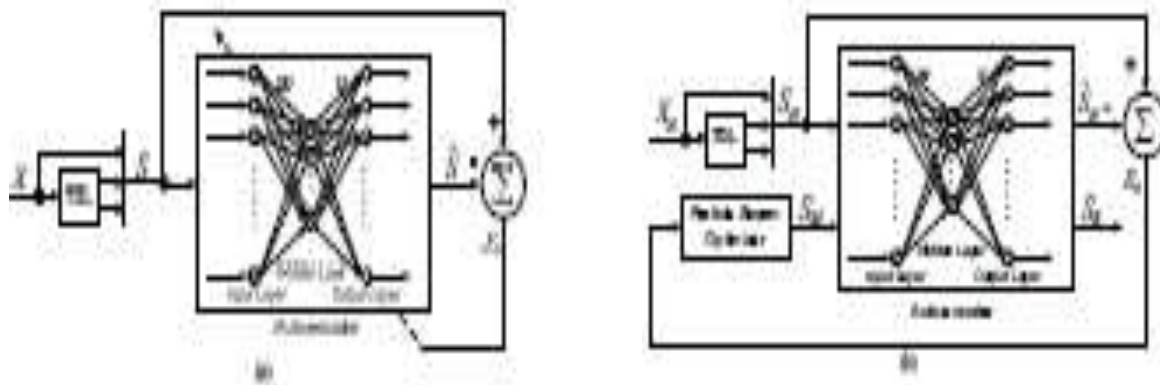


**Fig.4 Overall structure of MSR a) Training phase of the auto-encoder. b) On-line restoration of missing sensor data.**

1) *Auto-Encoder (Fig. 4(a))*: The auto-encoder is a multilayer perceptron (MLP) neural network with butterfly

structure [7], [8]. It has the same number of inputs and outputs, but the number of neurons in the hidden layer is less than that of the inputs. This particular structure creates a bottleneck in the feedforward path of the auto-encoder, enabling it to capture the correlations between the redundant inputs. The inputs of the auto-encoder,  $S$ , consist of the vector,  $X$ , at the present time step as well as at the previous two time steps (*i.e.*,  $S(k) = [X(k), X(k-1), X(k-2)]$ ). The use of the timedelayed inputs enables the auto-encoder to capture the auto-correlations of each variable in its input vector  $X$ . The auto-encoder is firstly trained without any missing sensor. During the training, the two PI controllers (PI<sub>d</sub>, PI<sub>q</sub>) are deactivated as shown in Fig. 3 and the steady state plant inputs  $v_{cqS}$  and  $v_{cdS}$  are disturbed by pseudorandom binary signals (PRBS) from an external source at each time step  $k$ , given by

$$PRBS_{v_{cd}}(k) = 0.1 |v_{cdS}| [\text{rand2}(k) + \text{rand3}(k) + \text{rand5}(k)] / 3 \quad (2)$$

$$PRBS_{v_{cq}}(k) = 0.1 |v_{cqS}| [\text{rand2}(k) + \text{rand3}(k) + \text{rand5}(k)] / 3 \quad (3)$$

where  $\text{rand2}$ ,  $\text{rand3}$  and  $\text{rand5}$  are uniformly distributed random numbers in  $[-1, 1]$  with frequencies 2 Hz, 3 Hz and 5 Hz, respectively;  $|v_{cdS}|$  and  $|v_{cqS}|$  are the magnitudes of  $v_{cdS}$  and  $v_{cqS}$  respectively. By feeding forward the data through the autoencoder and adjusting its weight matrices (using backpropagation algorithm),  $W$  and  $V$ , the auto-encoder is trained to map its inputs to its outputs. The detailed description of the auto-encoder training process has been given in [9].

## VI SIMULATION RESULTS

The dynamic performance of the proposed FTNC is evaluated at two different operating points by applying three phase short circuit and missing sensor tests.

### 6.1. Tests at the Operating Point Where Controllers are Designed

The RBFNC is trained and the CONVC is tuned at a specific operating condition (called OP-I), where the generator operates with a pre-fault rotor angle of  $42.6^\circ$ . A three-phase short circuit is applied to the receiving end of line 2 at  $t = 15$  s and 100 ms thereafter, line 2 is cleared out from the system. Three missing sensor tests are then applied from  $t = 15.1$  s during this post-fault transient state: 1) Case I –  $i_b$  missing; 2) Case II –  $i_b$  and  $i_c$  missing; 3) Case III –  $i_a$ ,  $i_b$  and  $i_c$  missing.

Figures 5,6 and7 show the results of the rotor angle  $\delta$  for Cases I, II and III, respectively. These results show that the damping control of the FTNC is more efficient than that of the CONVC during the post-fault transient state. During the first swing after the fault is applied, the FTNC is already providing significant damping compared to that provided by the CONVC. By continuously training the RBFNI and the RBFNC, the FTNC drives the plant successfully and quickly to a new operating point with a rotor angle  $\delta = 46.3^\circ$  at the steady state. Moreover, comparing the curves by FTNC with and without missing sensors, the transient performance of the FTNC only degrades slightly due to missing sensor data. However, comparing the curves CONVC and the curves FTNC with missing sensor or sensors, the transient

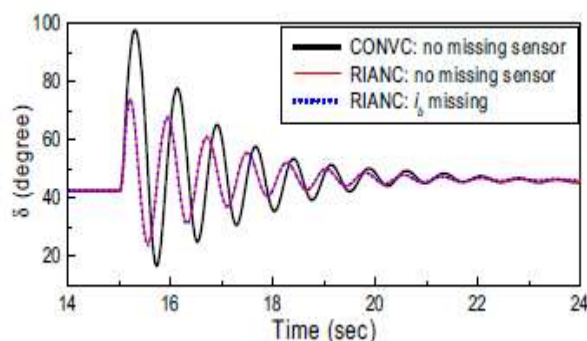


Fig.5. A 100ms three-phase short circuit at 15.0s at OP-I; case I- $i_b$  missing from 15.1s

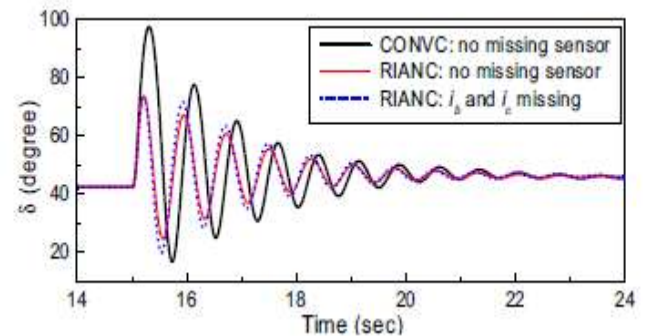
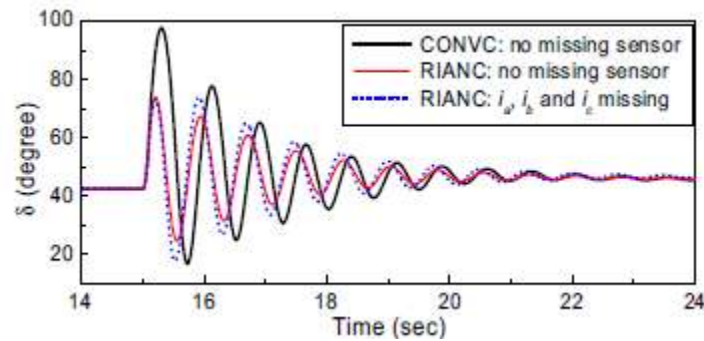


Fig.6. A 100ms three-phase short circuit at 15.0s at OP-I; Case II- $i_b$  and  $i_c$  missing from 15.1s.



**Fig.7 . A 100ms three-phase short circuit at 15.0s at OP-I; case III-ia ib and ic missing from 15.1s.**

performances of the FTNC with missing sensor measurements are still better than those of the CONVC used by the TCSC without any missing sensor. In this sense, the proposed FTNC provides a fault tolerant robust control for the TCSC.

## 6.2. Tests at a Different Operating Point

The transient performance of the FTNC is now re-evaluated at a different operating point (OP-II), where the pre-fault rotor angle of the generator changes to  $50.1^\circ$ ; line 1 is now open during this entire test. The parameters of the controllers are the same as those used in the test at OP-I, *i.e.*, the RBFNC has not been trained and the CONVC has not been tuned for OPII; but the SERS has been trained for this operating point. A 100 ms three-phase short circuit is applied to the receiving end of line 2 at  $t = 15$  s. Again, three missing sensor tests same as those in the previous subsection are applied during this postfault transient state.

Figures 8,9and 10 show the results of the rotor angle  $\delta$  for Cases I, II and III, respectively. These results indicate that the CONVC fails to drive the system back to the steady state after this large disturbance. However, the FTNC still provides the efficient control even if there are sensors missing or not. These results prove that the proposed FTNC provides improved transient performance over the CONVC and a faulttolerant control for the SSSC over a wide range of operating conditions. Under balanced operation, missing one sensor might be simply restored using the relationship  $ia + ib + ic = 0$ .However, the use of SERS is still necessary because it identifies which sensor is missing. This can not be achievedby only using that relationship. Moreover, power systems might experience unbalanced operations. In this case, the relationship above cannot be used to restore the missing sensor. The use of the SERS to identify and restore the missing sensors under unbalanced operating condition has been discussed and the simulation results have been given in [9].



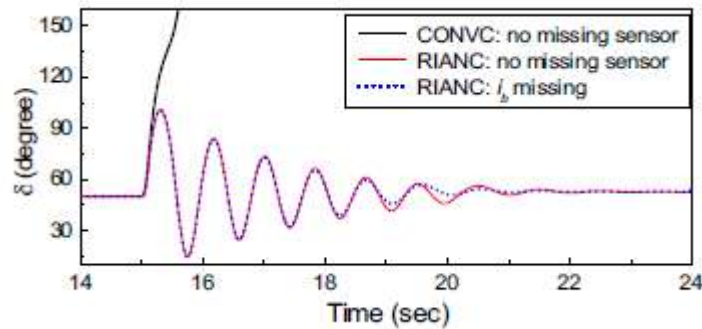


Fig.8 . A 100ms three-phase short circuit at 15.0s at OP-II; Case I- $i_b$  missing from 15.1s.

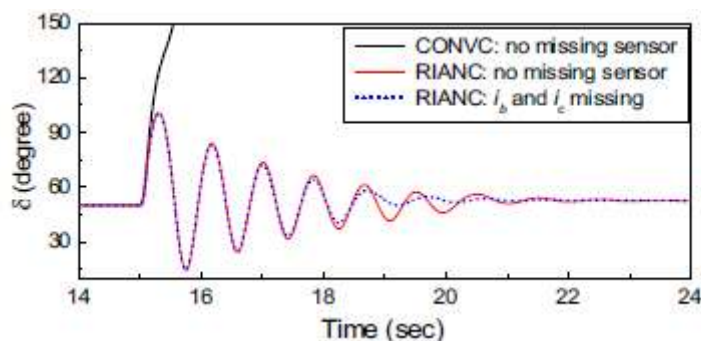


Fig.9. A 100ms three-phase short circuit at 15.0s at OP-II ; Case II- $i_b$  and  $i_c$  missing from 15.1s.

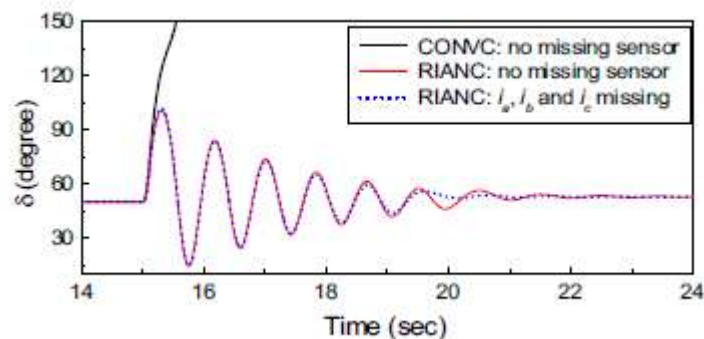


Fig.10. A 100ms three-phase short circuit at 15.0s at OP-II ; Case III –  $i_a$ ,  $i_b$  and  $i_c$  missing from 15.1s

## VII CONCLUSION

This paper has proposed a fault-tolerant indirect adaptive neuro-controller (FTNC) for the internal control of an TCSC, which combines a suitably designed sensor evaluation and (missing sensor) restoration scheme (SERS), a RBF neuroidentifier (RBFNI) and a RBF neuro-controller (RBFNC). The SERS is designed using the auto-

associative neural networks (auto-encoder). This FTNC is able to provide efficient control to the TCSC when some crucial sensor measurements are unavailable. Simulation studies are carried out at two operating conditions for the CONVC and the FTNC without any missing sensor, as well as for the FTNC with single and multiple phase current sensors missing; results show that the transient performances of the proposed FTNC with or without missing sensor measurements are both superior to the conventional linear PI controllers used by the TCSC without any missing sensor over a wide range of system operating conditions.

## REFERENCES

- [1] Johansson, NP, Nee H.P and Angquist L, "Estimation of Grid Parameters for the Control of Variable Series Reactance FACTS Devices", Proceedings of 2006 IEEE PES General Meeting
- [2] Johansson, N P, Nee H-P and Angquist L, "An Adaptive Model Predictive Approach to Power Oscillation Damping utilizing Variable Series Reactance FACTS Devices", Proceedings of the Universities Power Engineering Conference, Newcastle, UK, September 2006.
- [3] L. Zhang, M. L. Crow, Z. Yang, and S. Chen, "The steady state characteristics of an SSSC integrated with energy storage," in *Proc. 2001 IEEE Power Engineering Society Winter Meeting*, Jan. 28-Feb. 1, 2001, Columbus, OH, USA, vol. 3, pp. 1311-1316.
- [4] B. A. Renz, *et al*, "AEP unified power flow controller performance," *IEEE Trans. Power Delivery*, vol. 14, no. 4, pp. 1374-1381, Oct. 1999.
- [5] Bruce S. Rigby and R. G. Harley, "An improved control scheme for a series capacitive reactance compensator based on a voltage-source inverter," *IEEE Trans. Industry Applications*, vol. 34, no. 2, Mar./Apr.1998, pp. 355-363.
- [6] W. Qiao and R. G. Harley, "Indirect adaptive internal neuro-control for a static synchronous series compensator (SSSC) connected to a power system," in *Proc. the 31st Annual Conference of the IEEE Industrial Electronics Society*, Nov. 6-10, 2005, Raleigh, NC, USA, pp. 50-55.
- [7] M. A. El-Skarkawi and Robert J. Marks II, "Missing sensors restoration for system control and diagnostics," in *Proc. the 4th IEEE International Symposium on Diagnostics for Electric Machines, Power Electronics and Drives*, Aug. 24-26, 2003, Atlanta, GA, USA, pp. 338-341.
- [8] W. Qiao, Z. Gao, and R. G. Harley, "Continuous on-line identification of nonlinear plants in power systems with missing sensor measurements," in *Proc. 2005 International Joint Conference on Neural Networks*, July 31-Aug. 4, 2005, Montreal, QC, Canada, pp. 1729-1734.
- [9] W. Qiao, R. G. Harley and G. K. Venayagamoorthy, "A fault-tolerant PQ decoupled control scheme for static synchronous series compensator," to be presented at the *IEEE PES 2006 Annual Meeting*, Montreal, QC, Canada, June 18-22, 2006.